

Waterborne Fluorine-Free Superhydrophobic Surfaces Exhibiting Simultaneous CO₂ and Humidity Sorption

Avijit Baidya, Anagha Yatheendran, Tripti Ahuja, Chennu Sudhakar, Sarit Kumar Das, Robin H. A. Ras, and Thalappil Pradeep*

Recent progress in the field of superhydrophobic materials has proven their potential to solve many problems of the contemporary society. However, the use of such materials to capture moisture and CO₂ from air, to help reduce the impact of global climate change is not explored. In addition, most of the time, fabrication of these materials needs organic solvents and fluorinated molecules involving multiple steps that hinder the use of nonwetable materials in everyday life. Herein, a waterborne, fluorine-free, robust superhydrophobic material synthesized at room temperature through a one-step chemical-modification process is reported, which exhibits moisture and CO₂ capturing capability. While covalently grafted low surface energy hydrocarbon molecules control the bulk superhydrophobicity, the incorporated amine functionalities facilitate moisture and CO₂ adsorption as these molecules (H₂O and CO₂) can easily diffuse through hydrocarbon assemblies. Being polar, H₂O molecules are observed to readily interact with amine groups and favor the adsorption process. Synthesized material shows an approximate CO₂ adsorption of 480 ppm (10.90 mmol L⁻¹) in ambient conditions having 75% humidity. Multifunctionality along with durability of this material will help expand the applications of superhydrophobic materials.

1. Introduction

Mimicking natural phenomena is probably the best way to explore smartness. Over the years this has made Mother Nature an idol of architecture. Among many others, surfaces of various biological species having interesting nonwetting characteristics have attracted both industry and academia and have become some of the intensely pursued research areas because of their enormous potential in various domains.^[1] Although several methodologies have been introduced to fabricate these surfaces, complicated multistep processes, limitation in large area production, durability, etc., have restricted their use in everyday life.^[2] Recently, a few such robust liquid repelling surfaces have been reported.^[2c,3] However, in most of the cases, achieving such a property involves the use of 1) fluorine-containing chemicals (offering low surface energy) and 2) hazardous organic solvents.^[3a,4] While fluorinated hydrocarbons can lead to bioaccumulation and toxicity, the use of organic solvents increases environmental

concerns.^[5] Recently, a few superhydrophobic materials have also been designed with reduced environmental impact.^[6] For example, Chen and co-workers have demonstrated the fabrication of a fluorine-free robust superhydrophobic surface, but organic solvents were used in the process.^[7] We have shown the fabrication of organic-solvent-free superhydrophobic materials that contain fluorinated molecules.^[8] Therefore, designing a water-based fluorine-free robust low energy materials at ambient conditions is important from the perspective of reduced environmental impact and industrial significance.

Imparting new properties such as conductivity, chemical sensitivity, etc., especially to nonwetable materials is important.^[9] For example, introduction of carbon-based materials such as graphite, reduced-graphene, and carbon nanotubes to enhance the mechanical, thermal, and electrical conductivity,^[10] incorporation of inorganic nanoparticles such as TiO₂, and ZnO to impart biodegradation, etc.,^[2a,11] to superhydrophobic surfaces are well known. However, in most of the cases, these modified surfaces were developed through the incorporation of different micro/nanomaterials. In contrast, fabrication of superhydrophobic materials having molecularly grafted functionalities

Dr. A. Baidya, A. Yatheendran, T. Ahuja, C. Sudhakar, Prof. T. Pradeep
DST Unit of Nanoscience
Thematic Unit of Excellence
Department of Chemistry
Indian Institute of Technology Madras
Chennai 600036, India
E-mail: pradeep@iitm.ac.in

Dr. A. Baidya, Prof. R. H. A. Ras
Department of Applied Physics
Aalto University School of Science
Puumiehenkuja 2, 02150 Espoo, Finland

Dr. A. Baidya, Prof. S. K. Das
Department of Mechanical Engineering
Indian Institute of Technology Madras
Chennai 600036, India

Prof. R. H. A. Ras
Department of Bioproducts and Biosystems
Aalto University School of Chemical Engineering
Kemistintie 1, 02150 Espoo, Finland

 The ORCID identification number(s) for the author(s) of this article can be found under <https://doi.org/10.1002/admi.201901013>.

DOI: 10.1002/admi.201901013

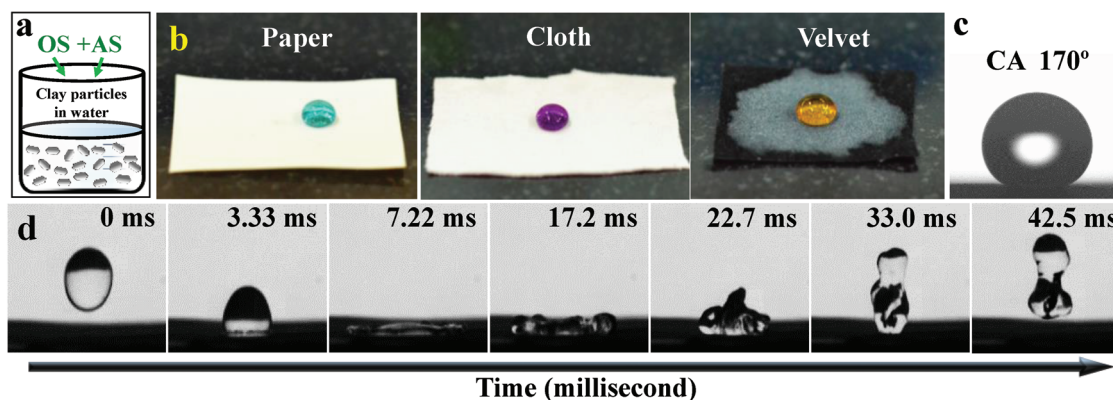


Figure 1. a) Schematic representation of the synthesis of a waterborne superhydrophobic material. b) Photograph of colored water droplets over various coated substrates. Aqueous solutions of CuCl_2 , KMnO_4 , and $\text{K}_2\text{Cr}_2\text{O}_7$ were used instead of pure water to add color contrast. c) Static water contact angle over a superhydrophobic paper. d) Time resolved bouncing of water droplet over a coated filter paper (soft surface).

to address various environmentally relevant problems has not been explored. In the context of recent concerns about the climate change, both moisture and CO_2 have great influence on the rise of atmospheric temperature. Although some superhydrophobic/omniophobic membranes^[12] and MOFs (metal organic frameworks)^[13] are known to capture CO_2 , their fabrication processes involve multiple steps, hazardous organic solvents, and fluorine-containing molecules. In the case of membranes, liquid repelling property enhances gas diffusion through them as the pores are not blocked by water molecules. CO_2 diffusion through the membranes is typically dissolved and separated by alkaline amine solutions.^[12a] For MOFs, even though it shows an uptake of $\approx 11.0 \text{ mol L}^{-1}$ at 298 K and 55 bar with 100 mg of the material, stability, complex fabrication protocols, bio and environmental-compatibility as well as industrial scale production require additional efforts. These limit the usability of these materials in everyday life even though they may possess good CO_2 adsorption capability.

Herein, we have designed an environment-friendly waterborne clay-based material at ambient conditions that provides a robust large-area superhydrophobic coating at room temperature and adsorbs moisture (water vapor) and CO_2 from air at the same time without affecting its nonwetting property. These multifunctional properties of the material arise from the covalently grafted chemical-functionalities having different molecular dimensions. While the incorporated hydrocarbon chain decreases the surface free energy of the material, amino functionalities (wrapped with clay sheets) facilitate adsorption of moisture and CO_2 through electronegative nitrogen atoms. Being synthesized and dispersed in water at neutral pH, it also minimizes the safety concerns, environmental pollution, and operational cost, enhancing industrial viability. Applicability of this material to develop a robust and flexible waterproof paper is also demonstrated and tested with various external perturbations. In short, herein a waterborne green superhydrophobic material is developed through a one-step wet-chemical process that possesses environmentally relevant multifunctional properties and shows potential applicability in various industries such as paints, packaging, clothing, and paper.

2. Results and Discussion

Figure 1a schematically represents one-pot chemical modification of native clay (NC) particles with two different types of silanes, octadecyltriethoxysilane (OS) and 3-(2-aminoethyl-amino)propyltrimethoxysilane (AS), at room temperature, in water. This results in excellent water-repelling thin films upon spray coating the suspension over various soft and hard substrates (Figure 1b). OS molecules, that possess low surface energy because of the hydrocarbon chain, get slowly adsorbed over clay sheets through hydroxyl groups and finally form covalent bonds through hydrolysis.^[8a] These hydrocarbon chains introduce nonwetting characteristics to the hydrophilic clay material that forced water droplet to sit as a sphere having a static contact angle (CA) of 170° (Figure 1c). Thermodynamically, it also minimizes the air–water–solid interfacial energy of water droplet and facilitates its rolling-off. Water-repelling property of the material was evaluated with advancing and receding contact angle (AC and RC) and contact angle hysteresis (CAH) measurements, which are more sensitive to the droplet dynamics on the surface (Figure S1, Supporting Information). This was further extended to droplet drag test (DDT) and vertical droplet adhesion test (VDAT)^[8a] (Figure S2 and Videos S1 and S2, Supporting Information). Bouncing of a water droplet even over a soft surface (coated filter paper) is pictorially presented in Figure 1d and Video S3 in the Supporting Information.

Modified clay (MC) induces nanoscale surface roughness, one of the prerequisites for superhydrophobicity, which was revealed through atomic force microscopy (AFM) (Figure 2a). While average surface roughness of the coated glass surface was $\approx 180 \text{ nm}$, NC coated glass surface showed an average roughness of 30 nm (Figure S3, Supporting Information). Such enhancement in roughness is known to be controlled by the hydrophobic effect,^[8a] namely an interaction between water and low surface energy molecules. Surface morphology of MC coated filter paper was imaged by scanning electron microscopy with a tilt angle of 45° (Figure S4, Supporting Information). Uniformly distributed nanoscale features over micrometer sized fibrous matrices facilitate the trapping of air, leading to an excellent water-repelling property. Inset demonstrates the

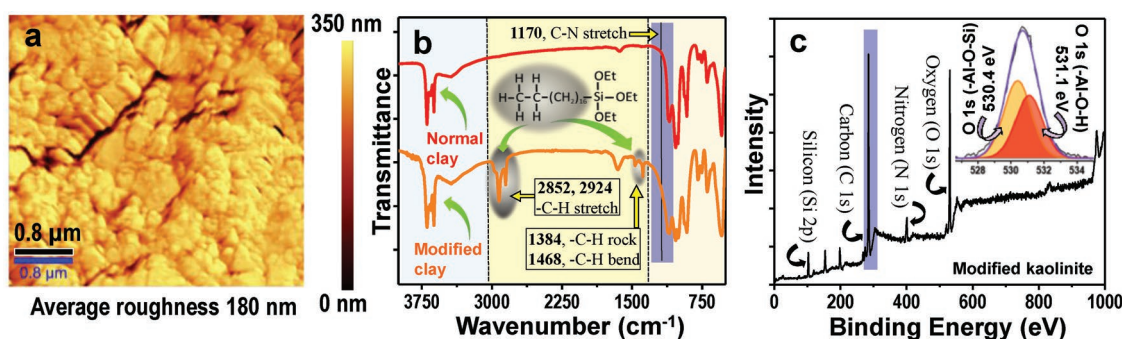


Figure 2. a) AFM image of the coated glass substrate reveals the roughness of the coating (average roughness 180 nm). b) IR spectra of the superhydrophobic material (normal and modified clay). Peaks at 2852, 2924, 1384, and 1468 cm^{-1} (marked area) correspond to various vibrational modes of the C–H bond. Shoulder at 1170 cm^{-1} (for expanded view, see Figure S6, Supporting Information), which broadened the spectrum, corresponds to C–N stretching. c) Survey and deconvoluted XPS spectra in the O1s region showing the relative concentrations of Al–O–H and Al–O–Si linkages, over chemically functionalized clay-coated surface.

top/perpendicular view (0°) of the surface. Figure S5 in the Supporting Information demonstrates the cross-sectional view of the layered superhydrophobic thin film, coated over a glass substrate. Average thickness of the coating was 8–10 μm .

Mode of attachment of the incorporated chemical-functionalities with NC particles, being the underlying reason to provide durable superhydrophobicity, was studied with IR spectroscopy and X-ray photoelectron spectroscopy (XPS). Additional peaks at 2852, 2924, 1384, and 1468 cm^{-1} (marked) in the IR spectrum of MC particles are related to the stretching, rocking and bending vibrational modes of the C–H bond (Figure 2b). This confirmed the chemical attachment of AS and OS with NC particles which is solely inorganic in nature (being an aluminosilicate). Apart from this, a shoulder at 1170 cm^{-1} (marked, expanded view Figure S6, Supporting Information), which is associated with the broadening of IR spectrum of MC in the region of 1100–1200 cm^{-1} , is related to the C–N stretching. NC particles (kaolinite) mostly consist of Al–O–H and Al–O–Si groups where the upper-most layer of the surface contains relatively higher concentration of Al–O–H (than Al–O–Si) groups (Figure S7, Supporting Information). These active O–H groups readily react with silane molecules resulting in an increase of Al–O–Si network over the surface. Figure 2c shows the relative concentrations of Al–O–H and Al–O–Si for the MC coated surface. Incorporation of hydrocarbon functionalities over the clay surfaces also reflects the presence of substantial amount of carbon (Figure 2c) compared to the unmodified one (Figure S8, Supporting Information). Small peak in the region of 285 eV in the spectrum of the NC corresponds to carbon, which mostly comes from the organic species (Figure S8, Supporting Information). Eventually, the covalent attachment between Si (from OS or AS) and OH (from NC) leads to the long-standing stability of the material. This was also tested by keeping both the as-synthesized MC dispersion and the coated substrates for 3 months at normal atmospheric condition and room temperature (30–38 $^\circ\text{C}$) (Experimental Section) in the laboratory condition.

Mechanical durability being an essential parameter toward various industrial applications, MC coated superhydrophobic surfaces were tested with several hard and soft abrasion tests. Static and dynamic contact angles of water droplets over abraded surfaces are graphically presented in Figure 3a. After

every ten completed abrasion cycles, water CA were measured and continued for 100 cycles. For instance, in the hard abrasion tests, the coated surface was subjected to sand paper abrasion test with a load of 50 g and mechanical-pressing test with a pressure of 264.4 atm (equivalent to a weight of 5 ton) (Figure S9i,ii, Supporting Information). In the first case, even though 100 abrasion cycles result in the removal of a few layers of the coating, the underlying layers helped to retain their water-repelling property intact^[8a,14] and made water droplets to roll-off through the abraded surface areas (Figure 3a). Similar water-repellent property was observed after mechanical-pressing test where the coated surface was subjected to a pressure of 264.4 atm (equivalent to a weight of 5 ton) (Figure S9ii, Supporting Information). For soft abrasions, the coated surface was tested with tissue paper abrasion and finger wiping test in a cyclic fashion (Figure S9iii,iv, Supporting Information). Here also, nonwettability was unchanged with spontaneous rolling-off of the water droplets through the abraded areas (Figure 3a). Unaltered superhydrophobicity of the abraded surface was further examined with DDT and VDAT. DDT over finger-wiped surface and VDAT over sand paper abraded surface are presented in Figure S10a,b and Videos S4 and S5 in the Supporting Information. To demonstrate the applicability of the material for various paper-based technologies, the coated superhydrophobic paper was subjected to various manual-bending-movements (Figure 3b,1–4) that are comparable to everyday applications. These were performed 100 times and the treated-surfaces were evaluated with CA and CAH measurements (Figure 3c). Durability of the coated surface was further tested with the oil-wash experiment (Figure S11, Supporting Information) where the superhydrophobic surface (filter paper) was artificially wetted with silicone oil and washed manually with ethanol and hexane. Retention of water-repelling characteristic upon the abovementioned experiments not only proves the durability of the material, it also showed the effective binding of the material with the substrate without any adhesive. This binding is due to the self-polymerization of secondary amine groups during the spontaneous drying process^[8a] that assists the binding between the clay particles as well as between the material and the substrate. These bending experiments also demonstrate the flexibility of the coated paper.

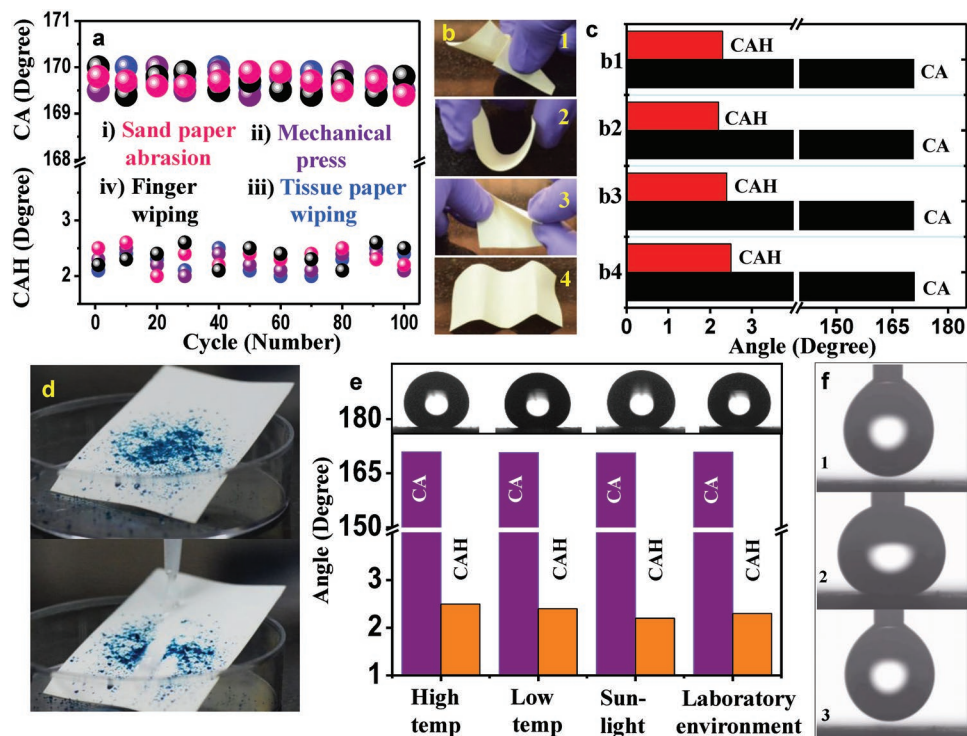


Figure 3. a) Durability of the water-repelling surface in terms of the change in CA and CAH of water droplet during multiple abrasion cycles. i) Sand paper abrasion with 50 g of load (abrasion distance of 5 cm), ii) mechanical pressing with a pressure of 264.4 atm (equivalent to the weight of 5 ton), iii) tissue paper abrasion, and iv) finger wiping test. b) Possible bending movements of the superhydrophobic paper (1)–(4). c) Change of nonwetting property of the superhydrophobic paper (presented through static CA and CAH) upon manual bending cycles illustrated in (b), for 100 times. d) Water-repelling and self-cleaning property of the coated paper after treating with an organic solvent (THF treated surface is demonstrated here). Water droplets carry the dust and roll off. e) Durability of the coated paper upon various environmental perturbations such as temperature treatments for 2 h (150 and $-80\text{ }^{\circ}\text{C}$), exposure to direct sunlight and normal laboratory environment for 3 months. Inset: Static contact angles of water droplet after corresponding experiments. f) Vertical droplet adhesion test over high-temp-treated superhydrophobic surface (1)–(3). Detachment of the water droplet without leaving any trace of water over the treated surface proves the retained nonwetting property of the coated substrate.

Similar to the mechanical durability, stability of the material toward low-surface-tension liquids that stick and penetrate the surface easily, was tested with multiple organic solvents having a range of polarity (Experimental Section). In the first case, surfaces were washed with different organic solvents and tested with the movement of water droplets after proper drying. In all the cases, surfaces were observed to maintain their superhydrophobicity and self-cleaning property. This is presented for tetrahydrofuran (THF)-treated surface in Figure 3d (pictorially) and Video S6 in the Supporting Information. In the second case, surfaces were immersed in selected solvents and kept for a long time (50 h) at room temperature in a closed container (to avoid the evaporation of the solvents). Water-repelling property of these surfaces was evaluated through CA and CAH measurements after every 5 h interval (Figure S12, Supporting Information). Behavior of acidic and basic ($\text{pH} = 1$ and $\text{pH} = 14$) water droplets over the coated surface was tested with CA measurements and VDATs (Figures S13 and S14, Supporting Information). Effect of various extreme environmental conditions such as high-temp ($150\text{ }^{\circ}\text{C}$), low-temp ($-80\text{ }^{\circ}\text{C}$), exposure to direct sunlight and normal laboratory conditions for long time were also tested in order to test the industrial relevance of this material (Figure 3e). Details are given in the Experimental Section. Inset shows the CA of the water droplet

after corresponding experiment. Treated surfaces were further tested with VDAT. Figure 3f and Video S7 in the Supporting Information correspond to VDAT over high-temp-treated surfaces. Temperature stability of the material was further investigated in detail till $250\text{ }^{\circ}\text{C}$ and the exposed surfaces were studied with CA and VDAT measurements (Figure S15a,b, Supporting Information). VDAT with $250\text{ }^{\circ}\text{C}$ temperature treated surface was presented in Figure S15b in the Supporting Information.

Apart from superhydrophobicity, the synthesized material showed interesting and environmentally relevant properties, such as adsorption of moisture and CO_2 . To demonstrate the moisture capturing ability of the material, coated filter papers were subjected to humid air (85% relative humidity, RH) in a closed container and change of RH with time was studied at constant temperature ($25\text{ }^{\circ}\text{C}$). Surprisingly, within 2 min, RH of the enclosure was seen to decrease to less than 20% (marked, Figure 4a) and finally reached a constant value of $(10 \pm 2)\%$ RH with time. This change in RH was not seen for filter paper and NC (Figure S16, Supporting Information). Amino-functionalities being the active sites to facilitate moisture-adsorption, along with the superhydrophobic material (AS + OS@clay) that contain AS, a control study was performed with only-amine functionalized clay (AS@clay) (Figure 4a, inset).

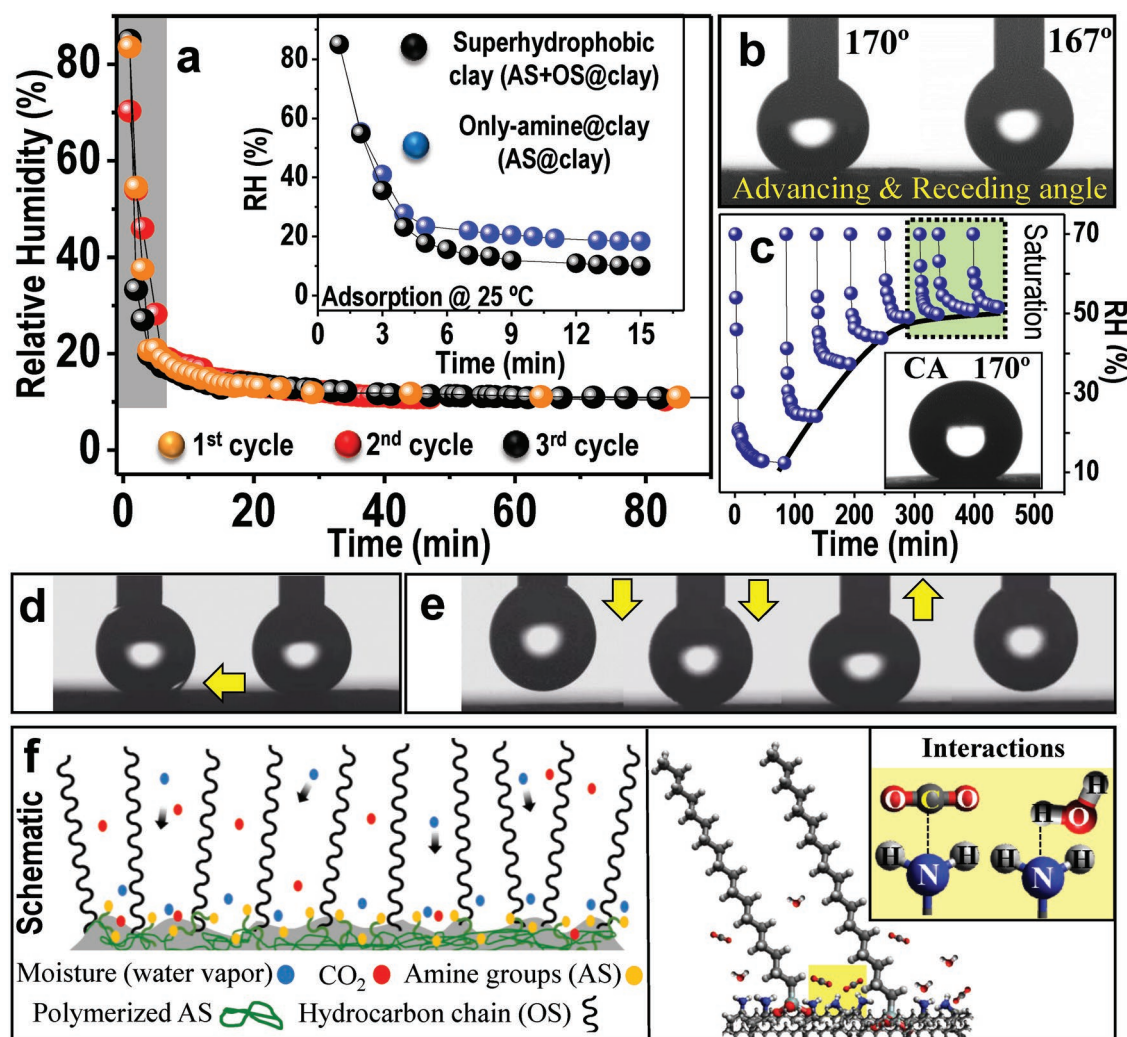


Figure 4. a) Rapid adsorption of moisture by superhydrophobic material at constant temperature. (Inset) Experiments with amine functionalized (AS@clay) and superhydrophobic (AS + OS@clay) surfaces prove that the amine functionalities are the underlying reason for moisture adsorption. Control experiment with NC is shown in Figure S16 in the Supporting Information. Both amine-functionalized clay and superhydrophobic clay contain the same amount of amine functionality. b) Advancing and receding water contact angles over superhydrophobic surface after the moisture-adsorption experiment (a). c) Consecutive cycles to achieve moisture saturation of the coated surface at constant temperature. Black curve represents the sigmoidal nature of moisture adsorption toward saturation. (Inset) Static CA of water droplet over saturated superhydrophobic surface derived from the experiment (c). d) Droplet drag test and e) vertical droplet adhesion test over moisture saturated superhydrophobic surface. f) A molecular-surface-functionality model to illustrate the moisture adsorption phenomenon over functional superhydrophobic material. Assembled hydrocarbon chains that control the bulk nonwettability (by decreasing surface energy and trapped air) but allow air molecules (moisture and CO₂) to diffuse into the assemblies. Inset: Interactions between electronegative nitrogen atom of amine group with water and CO₂.

Similar decrease of RH for both the cases revealed the moisture-adsorption mechanism as well as the importance of amino-functionalities to impart such a property to the coating material. Being an electronegative element, nitrogen atoms easily interact with water molecules through hydrogen bonds and facilitate adsorption of water. It is also possible through the electrostatic interaction between amine and water molecules, as secondary amine groups sometimes possess distinct positive charges. This reflects the fast adsorption kinetics of water molecules. Comparatively less adsorption of moisture for AS@clay compared to the AS + OS@clay, although concentration of amine-functionality was equal in both the materials, suggests that along with the presence

of active-chemical-functionalities, hydrophobic effect-induced enhancement of surface roughness (Figure 2a) results in higher surface exposure for the AS + OS@clay. However, the kinetics of this moisture adsorption was seen to be identical for both the materials, at constant temperature (25 °C). As surrounding temperature having a great influence on both RH and adsorption kinetics, temperature-dependent studies were performed with constant initial RH of 85% (Figure S17, Supporting Information) where negligible difference in the moisture adsorption was observed. Temperatures were chosen near indoor values. Although all these experiments were performed between 20 and 30 °C, rapid moisture adsorbing capability of the material is expected to be enhanced at lower surrounding temperatures.

Surprisingly, the water-repellent property of the material remained intact even after adsorption of moisture from air. Corresponding AC, RC, and CA over moisture adsorbed surfaces are presented in Figure 4b and Figure S18 in the Supporting Information. This was further studied in detail with a moisture-saturated superhydrophobic surface where the saturation-adsorption of the coated surface was carried out through multiple adsorption cycles at 25 °C, presented in Figure 4c. CA over this moisture-saturated sample was 170° (Figure 4c, inset), similar to the untreated surface (Figure 1c). Nonwettability of the moisture-saturated surface was also studied in detail with DDT and VDAT (Figure 4d,e and Video S8, Supporting Information). This can be correlated with the previously discussed experiments in Figure 3e where even after long exposure to sunlight and normal laboratory conditions (it results in the moisture-saturated surface), surfaces retain their water-repelling characteristics. For better understanding of such moisture adsorption phenomenon over a functional superhydrophobic material, a molecular-surface-functionality model is presented in Figure 4f. While small AS molecules get wrapped over the clay particles through a spontaneous self-polymerization of secondary amines, OS molecules with hydrocarbon chain mostly stay perpendicular to the surface^[15] and control the bulk nonwetting property of the surface by reducing the surface energy and by trapping air inside the assemblies. Although these assemblies restrict the penetration of water droplets, water vapor or moisture (blue dots) can easily diffuse between these giant molecular walls and get adsorbed with amine functionalities. Nitrogen

atom-induced interaction between amine functionalities and water molecules is shown in Figure 4f, inset. In short, the local molecular structure (and dimension) with proper chemical functionalities impart this property to the new superhydrophobic material.

For CO₂ capturing experiments, the coated surface was subjected to an artificially injected closed CO₂ environment. Figure 5a shows different cycles of CO₂ adsorption at 25 °C and a RH of 20%. Chemically, in this case also, molecular functionalities such as primary and secondary amines facilitate the adsorption of CO₂. This is schematically presented in Figure 4f where red color dots represent CO₂ molecules. Material shows an approximate CO₂ uptake of 480 ppm (10.90 mmol L⁻¹) under ambient conditions having 75% humidity. However, in this case, the adsorption kinetics was observed to be slower than the previous one (humidity adsorption). Unchanged wettability of the CO₂-adsorbed material was measured with CA (Figure 5a, inset). To identify the nature of chemical-bonding between CO₂ molecules and amine groups, CO₂-adsorbed material was characterized with IR spectroscopy (Figure 5b–d). As percentage of clay content is very high in the material and clay has various IR active modes in the lower region, only-amine (AS) which plays the key role to adsorb CO₂ was used to locate the chemical signatures related to the adsorption and interaction of CO₂ with amine groups (Figure 5b,c). Generally, CO₂ molecules bind with amine functionalities and form amide groups. Observed peak at 1650 cm⁻¹ relates to this C=O stretching of amides. Peaks at 1310 and 1412 cm⁻¹ correspond to the NCOO stretching

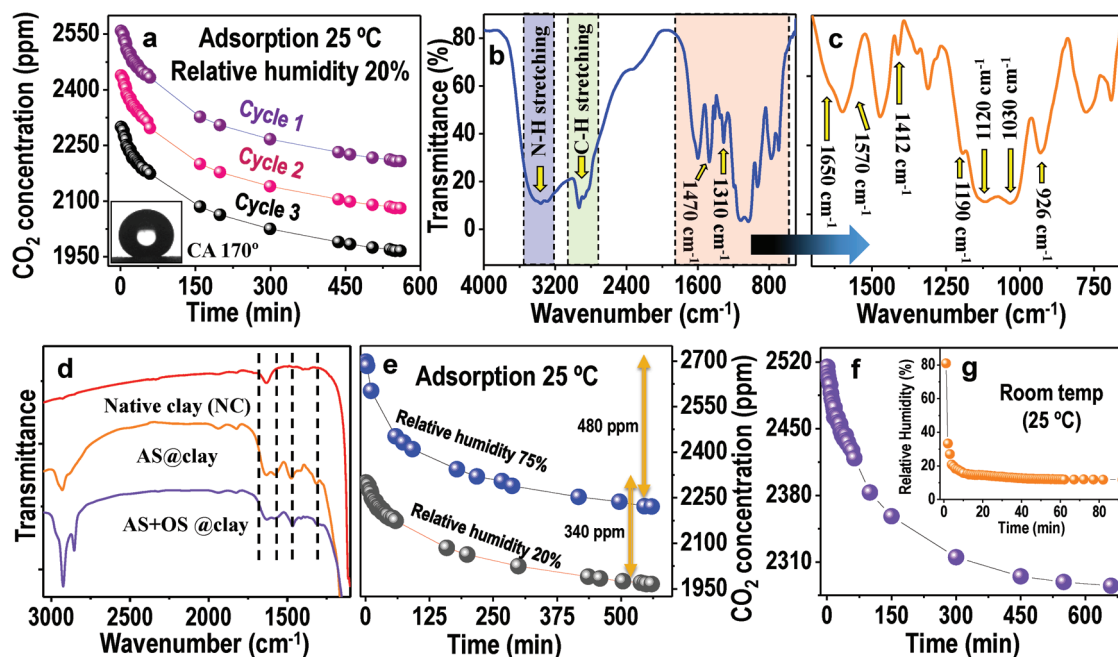


Figure 5. a) CO₂ capturing phenomenon over superhydrophobic surface at constant temperature. Inset: Static water contact angle over CO₂ adsorbed surface showing the retained superhydrophobicity of the coated substrates. b) IR spectrum of only-amine (AS) after CO₂ adsorption. As clay has different IR active sites (in lower region), to locate the chemical changes properly upon CO₂ adsorption, only-amine was used here. Signatures correspond to the uptake of CO₂ are marked. c) Enlarged view of the area of interest in the spectrum (b). d) IR spectra of CO₂-adsorbed native clay, amine-clay, and superhydrophobic clay. Characteristic features upon CO₂ adsorption are marked by dotted lines. These are present in both amine-clay and superhydrophobic clay but not observed in the IR spectrum of native clay. e) Influence of relative humidity on CO₂ adsorption process at constant temperature. f,g) Moisture and CO₂ adsorption performance (together) of the material at ambient conditions.

which also confirms the binding of CO₂ with amine functionalities. While peaks at 1030, 1120, and 1570 cm⁻¹ (shoulder) are associated with ammonium carbamate, peak at 1470 cm⁻¹ comes from NH₃⁺/NH₂⁺. Distinct peak at 926 cm⁻¹ relates to the N–H wagging of primary amine. However, these peaks are not present in pure amine.^[16] Figure 5d represents the IR spectra of CO₂-adsorbed NC, AS@clay, and AS + OS@clay, where none of the characteristic features of CO₂ adsorption were seen for NC (features due to CO₂ adsorption in AS@clay and AS + OS@clay are marked). Humidity being an influential parameter for chemical adsorption of CO₂, humidity dependent experiments were also performed at a constant temperature of 25 °C (Figure 5e). Adsorption of larger amount of CO₂ in higher RH (75%) compared to the low humid condition (20% RH) again validated the CO₂ capture mechanism of the material.^[17] While at low RH (25%), surface was observed to show adsorption of 350 ± 15 ppm CO₂, at RH 75% it was in the range of 480 ± 15 ppm CO₂ on an average. To demonstrate the real-life usability of the material, moisture and CO₂ capture experiments were performed together at constant temperature (Figure 5f,g). As seen before, in this case also, rapid adsorption of water vapor/moisture was observed and it decreased below 20% RH within a few minutes. At the same time, CO₂ capturing ability of the material remained unaltered. Having such important properties toward environmental issues along with its durable nonwettability, we believe that this multifunctional superhydrophobic material will enhance its usability in different technologies including paints, flexible electronics, and microfluidic devices.

3. Conclusion

In conclusion, we demonstrate the development of a green and multifunctional waterborne superhydrophobic material having an enhanced environmental relevance. Ability to adsorb moisture and CO₂ at the same time without affecting the water-repelling characteristics makes this material novel and industrially valuable. Being synthesized in water and ambient conditions, it promotes bulk production and minimizes additional environmental concerns and safety related issues. Durability of the coated surfaces against various external perturbations revealed the applicability of the material in day-to-day life. This includes various paper-based technologies, clothing, packaging, and many others. Molecular functionality-driven rapid adsorption of moisture at different temperatures promotes the versatile use of the material for different purposes. CO₂ adsorption capability even in dry condition highlights the potential of the material as well. Finally, the ease of synthesis and ecofriendly nature of the material not only broadens its industrial adoptability, it also addresses the urgent environmental need toward reducing the impact of air pollution and climate change.

4. Experimental Section

Materials: All the chemicals were purchased from commercial sources and used without further purification. Kaolinite clay was purchased from Alpha minerals and chemicals (India). OS (95%) was

purchased from Gelest (USA). AS (commercial grade) was purchased from Rishichem Distributors (India). Ethanol, hexane, heptane, dimethyl sulfoxide (DMSO), and THF were procured from RANKEM, India. All the chemicals were used without further purification. Sandpaper (P320) was purchased from a local hardware shop.

Synthesis: Chemical modification of the hydrophilic clay particles was performed solely in water through a wet chemical process (Figure 1a and Figure S19, Supporting Information). One pot synthesis of the material includes the mixing of two differently functionalized silane molecules, AS (1 mL) and OS (0.7 mL), with well-dispersed aqueous clay solution (2.75 wt%) at room temperature and was kept under vigorous stirring condition for 10–12 h. Although the silanes are generally very reactive in water, chemical attachment of OS with clay particles was controlled, as the solubility of OS in water is very low because of the long hydrophobic tail. Having silane functionality in another end, this low surface energy molecule initially gets adsorbed on the hydroxylated surfaces of clay particles and slowly underwent hydrolysis forming chemical bond with the clay sheet. As-synthesized dispersed material was then spray coated over various substrates and kept for drying. Although the coated surfaces were dried at room temperature (32 °C) and showed excellent water-repelling characteristic, to enhance the evaporation rate of water, coated substrates were also allowed to dry in warm condition (50 °C) that does not change the chemical and physical properties of the material (Figure S20, Supporting Information). Therefore, to prepare the bulk samples for multiple experiments, this condition (drying at 50 °C) was followed all the time.

Long Term Stability of the Material: Long-term stability of the material was tested through two different ways. In the first case, as synthesized material was immediately coated over the surfaces and kept for 3 months. In the second case, the synthesized material was stored for 3 months and then coated over the surfaces. In both the cases, surfaces showed similar water-repelling property compared to the freshly prepared samples (as-synthesized material immediately coated and dried). In addition, the stability of the chemical attachments of these molecules (AS and OS) with clay particles was also studied through IR spectroscopy. Here, the dried material was sonicated in water for 30 min and the supernatant was studied by IR spectroscopy (Figure S21, Supporting Information). In the Figure, spectrum of the supernatant (blue) does not contain any characteristic peak of either AS (black) and OS (red). Whereas the spectrum was similar to pure water (orange).

DDT and VDAT: For the drag test, a water droplet (≈5 μL) attached with a needle was dragged back and forth by 5 cm over a coated surface and the change was observed in the shape of droplet during the movement. Whereas in the second experiment, vertical droplet adhesion test, water droplet (≈5 μL) attached with a needle was moved up and down and pushed vertically over the surface to deform the shape of the droplet. Detachment of the water droplet from the superhydrophobic surface without leaving any traces showed the extent of the water-repelling nature of the material. These were performed in different locations of the surface as well.

Sand Paper Abrasion and Mechanical Pressing Test: For sand paper abrasion test, sand paper was placed between the surface and a load of 50 g and moved for 5 cm back and forth. After each ten consecutive cycles CA, AC, and RC of water droplet over abraded surface were measured and presented in Figure 3a. This was continued for 100 cycles. For mechanical pressing test, coated superhydrophobic paper was subjected to a pressure of 264.4 atm (equivalent to the weight of 5 ton). In this case, after every 1 h, CA, AC, and RC of water droplet was measured. This pressure treatment of 1 h corresponds to ten complete cycles.

Oil-Wash Experiment: For the oil-wash experiment, a coated filter paper was artificially wetted with viscous silicone oil. Being oleophilic in nature, oil adsorbs on the surface nicely and goes inside the rough surface structure. Adsorbed oil was then manually washed with ethanol and hexane. Washed filter paper was further kept inside hexane for 12 h and was tested with water after complete drying.

Chemical Durability Against Organic Solvents: Durability of the coated surface against organic solvent was performed in two ways with THF, DMSO, ethanol, and heptane. Solvents were chosen having different

polarity. In the first case, coated surfaces were washed with these solvents and tested with the movement of water droplets and self-cleaning property. For the second one, coated surfaces were immersed inside the organic solvents for 50 h in a closed container and tested with CA, AC, RC, and CAH measurements every 5 h intervals.

Durability against Environmental Stresses: Durability of the coated surface against various environmental stresses were evaluated by treating the surface with extreme temperature, direct sunlight, and normal laboratory atmosphere for long times. For temperature treatment, surfaces were kept at 150 °C and −80 °C for 2 h. Treated surfaces were tested with static and dynamic water contact angle measurements once they reached to ambient temperature. Change in wetting property of the surface upon exposure to sunlight and normal laboratory atmosphere for long time was tested by keeping the surfaces outside (under direct sunlight and laboratory environment) for 3 months. However, even after a year the surfaces were observed to retain their superhydrophobicity.

Temperature Stability Experiment: For studying the stability of the material at higher temperature (>150 °C), the coated surfaces were tested at 200, 225, and 250 °C. In all the cases, to eliminate the aerial oxidation, surfaces were heated in vacuum condition for 30 min. Nonwettability of the treated surfaces was examined with CA and VDAT. While till 250 °C, water droplets were observed to roll off nicely, above this, pinning of the droplets was seen.

Moisture and CO₂ Adsorption Experiments: Both moisture and CO₂ adsorption experiments were carried out with coated filter paper in a closed container at constant temperature (25 °C). On an average ≈1 g material was used to coat the filter papers. Reproducibility of such rapid moisture adsorption and CO₂ adsorption were studied with same coated filter paper for multiple time in a cyclic way. These are presented in Figures 4a and 5a. In between the experiments, coated surfaces were reactivated by desorbing the adsorbed water and CO₂ molecules at a relatively warm condition (50–60 °C) for 10 min.

Supporting Information

Supporting Information is available from the Wiley Online Library or from the author.

Acknowledgements

The authors thank the Department of Science and Technology, Government of India for constantly supporting this research program on nanomaterials. A.B. acknowledges support of INSPIRE Fellowship, Department of Science and Technology, Govt. of India. R.H.A.R. acknowledges support by European Research Council (ERC-2016-CoG No. 725513 “SuperRepel”) and the Academy of Finland Centres of Excellence Programme (2014–2019). This work was supported by Finnish National Agency for Education. The authors thank Prof. Mahesh V. Panchagnula for helping in bouncing of water droplets experiments.

Conflict of Interest

The authors declare no conflict of interest.

Keywords

environment-friendly, moisture sorption and CO₂ capture, robust, superhydrophobicity, waterborne

Received: June 10, 2019

Revised: July 22, 2019

Published online:

- [1] a) T. Sun, L. Feng, X. Gao, L. Jiang, *Acc. Chem. Res.* **2005**, *38*, 644; b) G. Kwon, E. Post, A. Tuteja, *MRS Commun.* **2015**, *5*, 475; c) Y. Zheng, H. Bai, Z. Huang, X. Tian, F.-Q. Nie, Y. Zhao, J. Zhai, L. Jiang, *Nature* **2010**, *463*, 640; d) M. P. Sousa, J. F. Mano, *ACS Appl. Mater. Interfaces* **2013**, *5*, 3731.
- [2] a) K. Liu, M. Cao, A. Fujishima, L. Jiang, *Chem. Rev.* **2014**, *114*, 10044; b) H. Teisala, M. Tuominen, J. Kuusipalo, *Adv. Mater. Interfaces* **2014**, *1*, 1300026; c) S. Wang, K. Liu, X. Yao, L. Jiang, *Chem. Rev.* **2015**, *115*, 8230; d) G. B. Hwang, K. Page, A. Patir, S. P. Nair, E. Allan, I. P. Parkin, *ACS Nano* **2018**, *12*, 6050.
- [3] a) C. Peng, Z. Chen, M. K. Tiwari, *Nat. Mater.* **2018**, *17*, 355; b) J. E. Mates, T. M. Schutzius, I. S. Bayer, J. Qin, D. E. Waldroup, C. M. Megaridis, *Ind. Eng. Chem. Res.* **2014**, *53*, 222; c) D. Soto, A. Ugur, T. A. Farnham, K. K. Gleason, K. K. Varanasi, *Adv. Funct. Mater.* **2018**, *28*, 1707355.
- [4] a) Y. Lu, S. Sathasivam, J. Song, C. R. Crick, C. J. Carmalt, I. P. Parkin, *Science* **2015**, *347*, 1132; b) L. Li, B. Li, J. Dong, J. Zhang, *J. Mater. Chem. A* **2016**, *4*, 13677; c) X. Deng, L. Mammen, H.-J. Butt, D. Vollmer, *Science* **2012**, *335*, 67; d) X. Du, M. Wang, A. Welle, F. Behboodi-Sadabad, Y. Wang, P. A. Levkin, Z. Gu, *Adv. Funct. Mater.* **2018**, *28*, 1803765; e) D. Yoo, Y. Kim, M. Min, G. H. Ahn, D.-H. Lien, J. Jang, H. Jeong, Y. Song, S. Chung, A. Javey, T. Lee, *ACS Nano* **2018**, *12*, 11062; f) S. Pan, R. Guo, M. Björnalm, J. J. Richardson, L. Li, C. Peng, N. Bertleff-Zieschang, W. Xu, J. Jiang, F. Caruso, *Nat. Mater.* **2018**, *17*, 1040.
- [5] a) K. Chen, S. Zhou, S. Yang, L. Wu, *Adv. Funct. Mater.* **2015**, *25*, 1035; b) T. Darmanin, F. Guittard, *Soft Matter* **2013**, *9*, 5982.
- [6] a) A. M. Rather, U. Manna, *ACS Appl. Mater. Interfaces* **2018**, *10*, 23451; b) Z.-h. Zhang, H.-j. Wang, Y.-h. Liang, X.-j. Li, L.-q. Ren, Z.-q. Cui, C. Luo, *Sci. Rep.* **2018**, *8*, 3869.
- [7] H. Ye, L. Zhu, W. Li, H. Liu, H. Chen, *ACS Appl. Mater. Interfaces* **2017**, *9*, 858.
- [8] a) A. Baidya, M. A. Ganayee, S. Jakka Ravindran, K. C. Tam, S. K. Das, R. H. A. Ras, T. Pradeep, *ACS Nano* **2017**, *11*, 11091; b) A. Baidya, S. K. Das, R. H. A. Ras, T. Pradeep, *Adv. Mater. Interfaces* **2018**, *5*, 1701523.
- [9] a) Y. Ren, Z. Lin, X. Mao, W. Tian, T. Voorhis, T. A. Hatton, *Adv. Funct. Mater.* **2018**, *28*, 1801466; b) R. Wang, J. Zhu, K. Meng, H. Wang, T. Deng, X. Gao, L. Jiang, *Adv. Funct. Mater.* **2018**, *28*, 1800634; c) V. Jokinen, E. Kankuri, S. Hoshian, S. Franssila, R. H. A. Ras, *Adv. Mater.* **2018**, *30*, 1705104.
- [10] a) Y. C. Jung, B. Bhushan, *ACS Nano* **2009**, *3*, 4155; b) L. Ye, J. Guan, Z. Li, J. Zhao, C. Ye, J. You, Y. Li, *Langmuir* **2017**, *33*, 1368; c) A. Das, J. Deka, A. M. Rather, B. K. Bhunia, P. P. Saikia, B. B. Mandal, K. Raidongia, U. Manna, *ACS Appl. Mater. Interfaces* **2017**, *9*, 42354; d) K. K. Jung, Y. Jung, C. J. Choi, J. S. Ko, *ACS Omega* **2018**, *3*, 12956.
- [11] L. Chen, X. Sheng, D. Wang, J. Liu, R. Sun, L. Jiang, X. Feng, *Adv. Funct. Mater.* **2018**, *28*, 1801483.
- [12] a) F. Geyer, C. Schönecker, H.-J. Butt, D. Vollmer, *Adv. Mater.* **2017**, *29*, 1603524; b) Y.-F. Lin, W.-W. Wang, C.-Y. Chang, *J. Mater. Chem. A* **2018**, *6*, 9489.
- [13] a) C. Serre, *Angew. Chem., Int. Ed.* **2012**, *51*, 6048; b) P. Z. Moghadam, J. F. Ivy, R. K. Arvapally, A. M. dos Santos, J. C. Pearson, L. Zhang, E. Tylianakis, P. Ghosh, I. W. H. Oswald, U. Kaipa, X. Wang, A. K. Wilson, R. Q. Snurr, M. A. Omary, *Chem. Sci.* **2017**, *8*, 3989.
- [14] T. Verho, C. Bower, P. Andrew, S. Franssila, O. Ikkala, R. H. A. Ras, *Adv. Mater.* **2011**, *23*, 673.
- [15] C. Nicosia, J. Huskens, *Mater. Horiz.* **2014**, *1*, 32.
- [16] S. Ek, E. I. Iiskola, L. Niinistö, *J. Phys. Chem. B* **2004**, *108*, 9650.
- [17] a) J. J. Lee, C.-H. Chen, D. Shimon, S. E. Hayes, C. Sievers, C. W. Jones, *J. Phys. Chem. C* **2017**, *121*, 23480; b) A. Gholidoust, J. D. Atkinson, Z. Hashisho, *Energy Fuels* **2017**, *31*, 1756.